Acta Crystallographica Section C
Crystal Structure Communications
ISSN 0108-2701

A structural systematic study of four isomers of difluoro-*N*-(3-pyridyl)-benzamide

Joyce McMahon,[a] John F. Gallagher,[a]* Frankie P. Anderson[b] and Alan J. Lough[c]

[a]School of Chemical Sciences, Dublin City University, Dublin 9, Ireland, [b]National Institute for Cellular Biotechnology, School of Chemical Sciences, Dublin City University, Dublin 9, Ireland, and [c]Department of Chemistry, 80 St George Street, University of Toronto, Toronto, Ontario, Canada M5S 3H6
Correspondence e-mail: john.gallagher@dcu.ie

Received 4 June 2009
Accepted 10 June 2009
Online 27 June 2009

The four isomers 2,4-, (I), 2,5-, (II), 3,4-, (III), and 3,5-difluoro-*N*-(3-pyridyl)benzamide, (IV), all with formula $C_{12}H_8F_2N_2O$, display molecular similarity, with interplanar angles between the C_6/C_5N rings ranging from 2.94 (11)° in (IV) to 4.48 (18)° in (I), although the amide group is twisted from either plane by 18.0 (2)–27.3 (3)°. Compounds (I) and (II) are isostructural but are not isomorphous. Intermolecular N—H···O=C interactions form one-dimensional *C*(4) chains along [010]. The only other significant interaction is C—H···F. The pyridyl (py) N atom does not participate in hydrogen bonding; the closest $H\cdots N_{py}$ contact is 2.71 Å in (I) and 2.69 Å in (II). Packing of pairs of one-dimensional chains in a herring-bone fashion occurs *via* π-stacking interactions. Compounds (III) and (IV) are essentially isomorphous (their *a* and *b* unit-cell lengths differ by 9%, due mainly to 3,4-F_2 and 3,5-F_2 substitution patterns in the arene ring) and are quasi-isostructural. In (III), benzene rotational disorder is present, with the *meta* F atom occupying both 3- and 5-F positions with site occupancies of 0.809 (4) and 0.191 (4), respectively. The $N—H\cdots N_{py}$ intermolecular interactions dominate as *C*(5) chains in tandem with $C—H\cdots N_{py}$ interactions. C—H···O=C interactions form $R_2^2(8)$ rings about inversion centres, and there are π–π stacks about inversion centres, all combining to form a three-dimensional network. By contrast, (IV) has no strong hydrogen bonds; the $N—H\cdots N_{py}$ interaction is 0.3 Å longer than in (III). The carbonyl O atom participates only in weak interactions and is surrounded in a square-pyramidal contact geometry with two intramolecular and three intermolecular C—H···O=C interactions. Compounds (III) and (IV) are interesting examples of two isomers with similar unit-cell parameters and gross packing but which display quite different intermolecular interactions at the primary level due to subtle packing differences at the atom/group/ring level arising from differences in the peripheral ring-substitution patterns.

Comment

Structural systematic studies are at the core of drug-design programmes. The ability to synthesize and study closely related compounds and then monitor and correlate their chemical or biological effects in guest–host interactions is at the heart of understanding how small molecules (guests or drugs) interact with biological hosts as potential novel inhibitors or activators. In structural chemistry, a multitude of crystal structure studies have been reported to date on a variety of organic molecular classes and with a particular emphasis on polymorphism, pseudopolymorphism and isomers (Gelbrich *et al.*, 2007; Wardell *et al.*, 2007, 2008; Chopra & Row, 2008). The variety and sizes of structural series reported are expanding rapidly and notable examples include benzoate esters (Gowda, Foro, Sowmya & Fuess, 2008) and both mono/dimethyl- and chlorobenzamides (Gowda, Foro, Babitha & Fuess, 2008). Series such as these provide a 'goldmine' of structural data for ongoing data analyses.

Our group has recently initiated a systematic structural study of (mono/di)fluoro-*N*′-pyridylbenzamide isomers (Donnelly *et al.*, 2008; Gallagher *et al.*, 2008; McMahon *et al.*, 2008). In the difluoro-*N*-pyridylbenzamide series (see first scheme), a total of 18 isomers are possible through condensation of the 2,3-, 2,4-, 2,5-, 2,6-, 3,4- and 3,5-difluorobenzoyl chlorides with the 4-, 3- or 2-aminopyridines. We have reported four isomers to date, namely the 23*p*, 24*p*, 25*p* and 23*o* derivatives, where the digits 2–6 represents the F_2 substitution pattern on the benzene ring and *p*, *m* and *o* represent the N-atom pyridine ring position with respect to the amide group (McMahon *et al.*, 2008; Gallagher *et al.*, 2008). We report herein the molecular and crystal structures of the isomers 2,4-difluoro-*N*′-(3-pyridyl)benzamide, (I), 2,5-difluoro-*N*′-(3-pyridyl)benzamide, (II), 3,4-difluoro-*N*′-(3-pyridyl)benzamide, (III), and 3,5-difluoro-*N*′-(3-pyridyl)benzamide, (IV).

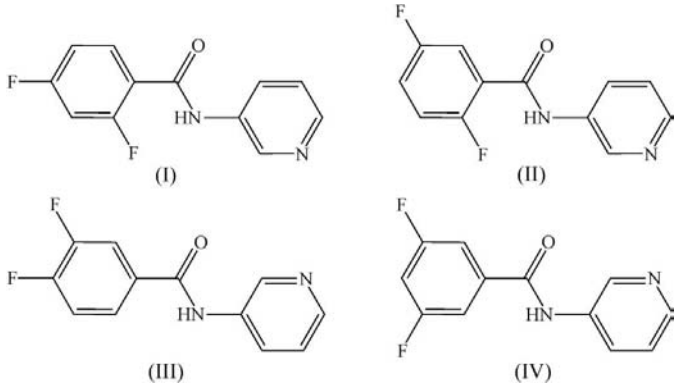

The four isomers (I)–(IV) are depicted in Figs. 1–4, and in the packing diagrams (Figs. 6–9) and molecular overlays (Figs. 10 and 11). The geometric data (bond lengths and angles) are normal and are not discussed, except for comparisons with

 doi:10.1107/S010827010902215X

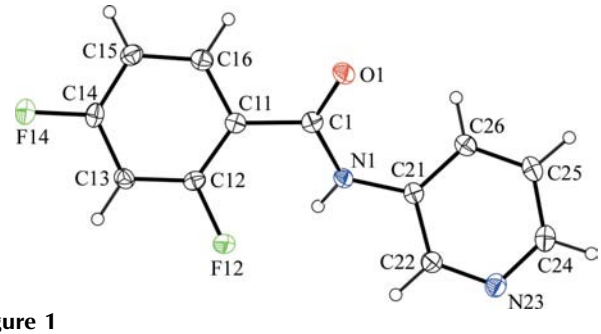

Figure 1
A view of (I), showing the atomic numbering scheme. Displacement ellipsoids are drawn at the 30% probability level and H atoms are shown as small spheres of arbitrary radii.

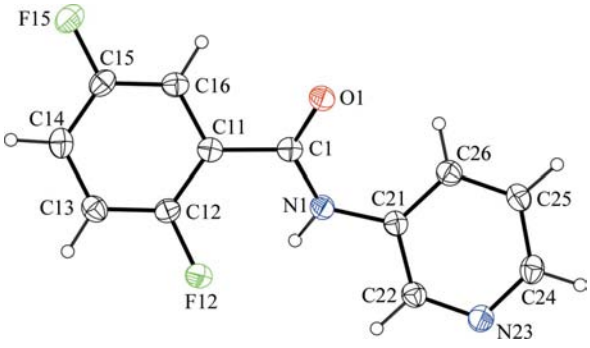

Figure 2
A view of (II), showing the atomic numbering scheme. Displacement ellipsoids are drawn at the 30% probability level and H atoms are shown as small spheres of arbitrary radii.

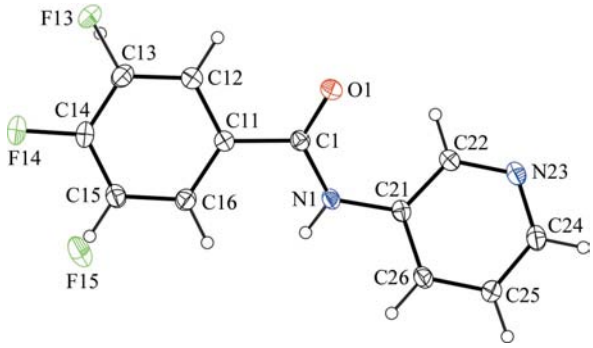

Figure 3
A view of (III), showing the atomic numbering scheme. Displacement ellipsoids are drawn at the 30% probability level and H atoms are shown as small spheres of arbitrary radii. The disordered F atoms F13/F15 are depicted with the alternating H atoms.

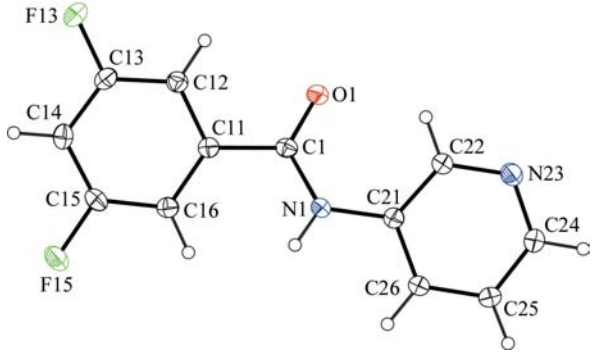

Figure 4
A view of (IV), showing the atomic numbering scheme. Displacement ellipsoids are drawn at the 30% probability level and H atoms are shown as small spheres of arbitrary radii.

related systems (Fig. 5), and the hydrogen-bonding/packing interactions (Tables 1–4) and torsion/interplanar angles (Table 5). Differences in bond lengths and angles between the four structures are typically <0.02 Å and <2°, respectively, and are influenced by the position of the F-atom substitution pattern on both the *ipso* (at F-atom sites) and *ortho* (to F) C—C—C angles; they are typical of the F-atom ring location (Luthe *et al.*, 2007; Klösener *et al.*, 2008). In (III), benzene rotational disorder is observed in the 3,4-difluorobenzene group, with the 3-F atom occupying both 3- and 5-F atom positions, with site occupancies of 0.809 (4) and 0.191 (4), respectively, for the major and minor components of disorder. Interestingly, a molecular difference between the (I)/(II) and (III)/(IV) pairs is that the C═O group and N atoms are oriented *transoid* to each other in the former and *cisoid* in the latter (Figs. 1–4; see also first scheme).

The defining feature of the molecular conformation in these four isomers is the dihedral angle between the benzene and pyridine rings, which are mutally oriented at between 4.48 (18)° in (I) and 2.94 (11)° in (IV) (Figs. 1–4 and Table 5), while the three-atom amide unit is rotated by < 30° from either the six-membered C_6 or C_5N plane [18.0 (2)–27.3 (3)° for all four structures]. An overlay of (I) and (II) (Fig. 10) highlights the similar conformations for the two structures, and Fig. 11 shows an overlay of (III) and (IV). In (I) and (II), the *ortho*-F atom is positioned *transoid* to the carbonyl O atom, with two intramolecular contacts involving C26···O1 and N1···F12 [both with *S*(6) motifs; Bernstein *et al.*, 1995]. The C26···O1 distances are invariant, at 2.910 (3) Å in (I) and 2.913 (3) Å for (II) [C—H···O = 113° for both (I) and (II)]. However, N1···F1 varies slightly from 2.741 (3) Å in (I) to 2.726 (2) Å in (II), with angles of 117 (2)° in (I) and 123 (2)° in (II) as the C1—N1—C21—(C22/C26) torsion angle decreases (Table 5).

Compounds (III) and (IV) are essentially isomorphous (their *a* and *b* unit-cell lengths differ by 9%) and are quasi-isostructural at the primary hydrogen-bonding level. Overlay of the unit cells indicates that (III) and (IV) occupy similar three-dimensional volume elements within their respective unit cells but that the atoms (and rings) are sufficiently displaced in each molecular structure to effect a packing situation whereby the N—H group involved in a strong interaction in (III) only forms a weaker analogous interaction in (IV) (Fig. 11). Differences arise principally from the steric effects of the 3,4-F_2 (disordered) and 3,5-F_2 substitution patterns at the molecular sites on the packing and resultant unit-cell parameters. The 3,5-F_2 group causes a longer *a* dimension in (IV) and the 4-F substitution in (III) lengthens *b*, with a resulting impact on the observed and different geometric values of the principal N—H···N interaction. A variable-temperature study would be useful to ascertain how similar the crystal structures of (III) and (IV) are over a range of temperatures; Threlfall & Gelbrich (2007) have described

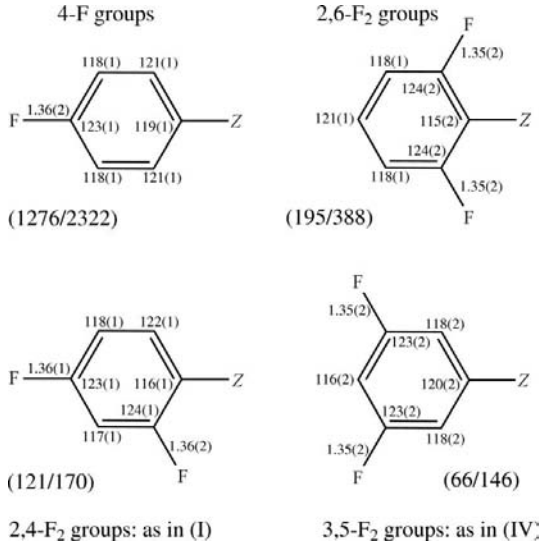

Figure 5
The geometry of the 4-fluorobenzene and 2,4-, 2,6- and 3,5-difluorobenzene fragments. Analysis of the CSD (Allen, 2002) with three-dimensional coordinates, no restrictions and with Z = any atom but hydrogen. H atoms, though not depicted, were included in the CSD analysis.

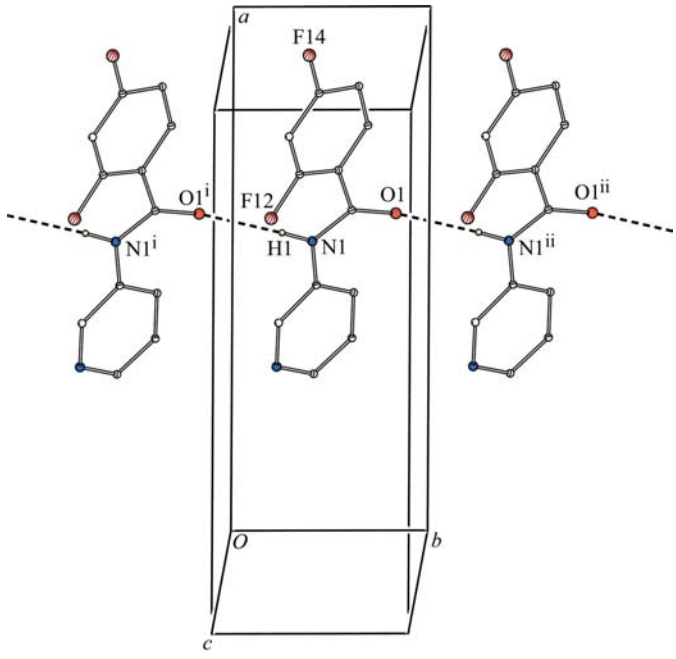

Figure 6
The primary N—H···O═C interaction in (I), forming a $C(4)$ chain along [010]. H atoms not involved in hydrogen bonding have been omitted for clarity. [Symmetry codes: (i) $x, y-1, z$; (ii) $x, y+1, z$.]

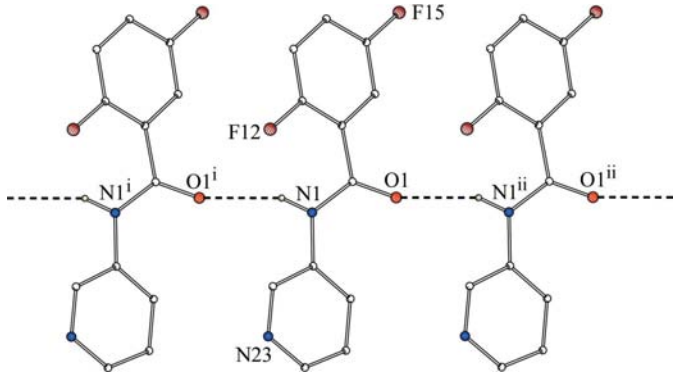

Figure 7
The primary N—H···O═C interaction in (II), forming a $C(4)$ chain. Symmetry codes are as in Fig. 6. H atoms not involved in hydrogen bonding have been omitted for clarity.

the pitfalls of accrediting great significance to structural differences which can be readily explained by normal changes of lattice expansion over a range of temperatures.

For a comparison of structures (I)–(IV) with literature data, a survey and analysis of the relevant bond lengths and angles was undertaken. Luthe and co-workers have reported a comprehensive study of fluorinated 4-chlorobiphenyls (PCB 3) (Luthe *et al.*, 2007) and 4-bromodiphenyl ethers (PBDE 3) (Klösener *et al.*, 2008), where the interior aromatic C—C—C ring angles (due to the *ipso*-F position) are shown to increase by 2–3° (or decrease from 120° for *ortho*-related angles) from the ideal value of 120°, as also demonstrated by computational calculations at the 3–21 level using *SPARTAN* (Shao *et al.*, 2006). The *ipso* ring-angle increase is attributed to hyperconjugation of the fluorine 2*p* orbitals with the π-orbitals of the aromatic ring system; neighbouring (*ortho*) C—C—C ring angles deviate from 120° to compensate. The effect of fluorine 'tagging' has an impact on the internal aromatic angles, dihedral angles, packing and neighbouring groups, although less than for Cl substitution (Luthe *et al.*, 2007; Klösener *et al.*, 2008).

The 4-fluorophenyl FC_6H_4-Z moiety (Z = any atom but H) was selected as a model group, giving 1276 hits (2322 observations; see Fig. 5) in a search of the Cambridge Structural Database (CSD, Version 5.30 plus two updates; Allen, 2002). The *ipso*-F angle for 4-F derivatives expands to 123 (1)°, while angles *ortho* to F contract to 118 (1)° [*meta* angles to F increase slightly to 121 (1)°]. Analysis of the C—F bond lengths with *ipso*-C—C—C angles shows a trend line whereby increasing C—F bond lengths (from 1.35 to 1.38 Å) correlate well with increasing C—C—C angles (from 120 to 126°). Influences include the effects of both intra- and intermolecular interactions on the F-atom geometric data. The F-atom position on the aromatic ring influences distinct geometric patterns at both the *ipso* and *ortho* C—C—C angles (Fig. 5). The molecular analysis results and calculations (Luthe *et al.*, 2007; Klösener *et al.*, 2008) agree with both our CSD analysis and previous results from the 4-/3-/2-fluoro-*N*′-(4-pyridyl)benzamides (Donnelly *et al.*, 2008), where 4–5° differences in the internal aromatic C—C—C angles are observed.

This F-atom effect was analysed for related $C_6H_3F_2-Z$ moieties in the CSD for comparison with the 4-F study (above) and compounds (I)–(IV). Difluorobenzene fragments are rare in structural chemistry (Fig. 1 in McMahon *et al.*, 2008) compared with the vast plethora of both mono-substi-

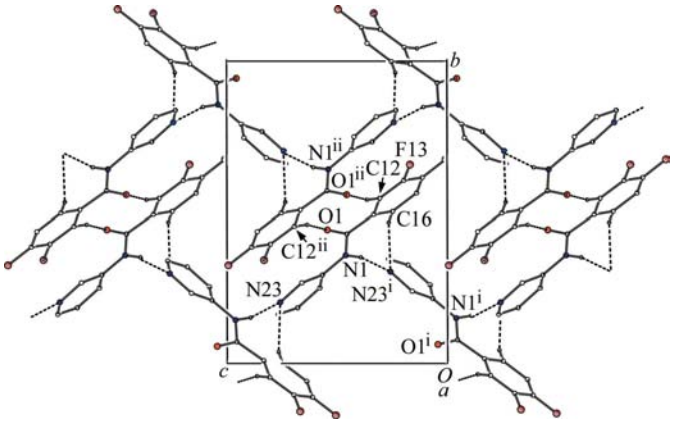

Figure 8
The primary N—H···N interactions in the unit cell of (III), forming $C(5)$ chains as viewed along [100]. H atoms not involved in hydrogen bonding have been omitted for clarity. Chains are linked about inversion centres by C—H···O interactions with an $R_2^2(10)$ motif. [Symmetry codes: (i) $x-\frac{1}{2}$, $-y+\frac{1}{2}$, $z-\frac{1}{2}$; (ii) $2-x$, $1-y$, $1-z$.]

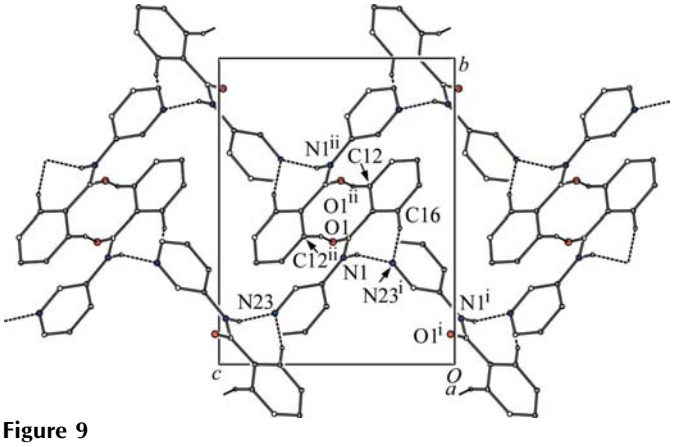

Figure 9
The primary N—H···N interactions in the unit cell of (IV), forming $C(5)$ chains as viewed along [100]. H atoms not involved in hydrogen bonding, as well as all F atoms, have been omitted for clarity. Chains are linked about inversion centres by C—H···O interactions with an $R_2^2(10)$ motif. [Symmetry codes: (i) $x-\frac{1}{2}$, $-y-\frac{1}{2}$, $z-\frac{1}{2}$; (ii) $2-x$, $1-y$, $1-z$.]

tuted fluoro- and pentafluorobenzene derivatives reported in the CSD (Allen, 2002).

Analysis of the 2,3-, 2,4-, 2,5-, 2,6-, 3,4- and 3,5-difluorobenzene groups in the CSD provides indicators for particular trends and for comparisons with (I)–(IV), but the data available are too few to allow comprehensive comparisons in three cases, namely the 2,3- (with 15 structures out of 17 observations), 2,5- (with 28/40 data) and 3,4- (with 30/48 data) structures. The CSD data for the 2,4-difluorobenzene fragment (121/170 data), and 2,6- (195/388 data) and 3,5-disubstituted fragments (66/146 data), provide average C—F bond lengths of 1.35 Å and *ca* 4–5° differences in the internal C—C—C angles, depending on whether the F is *ipso* (with C—C—C > 120°) or *ortho* (with C—C—C < 120°) (Fig. 5).

Analysis of the 2,4-difluorobenzene fragment in the CSD gives typical C—F bond lengths of 1.36 (1) Å, comparable with the values of 1.365 (3) and 1.359 (3) Å in (I). The variation in internal C—C—C angles within the 2,4-difluoro-

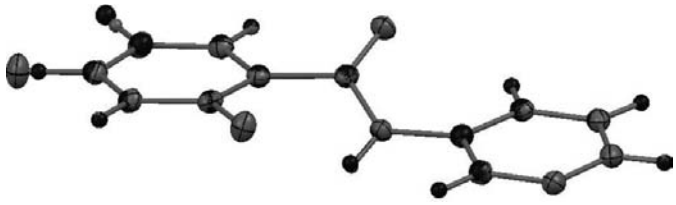

Figure 10
An overlay of (I) (grey) and (II) (black), highlighting the molecular similarity. Atoms in (I) are depicted as displacement ellipsoids at the 30% probability level and for (II) using a ball-and-stick model.

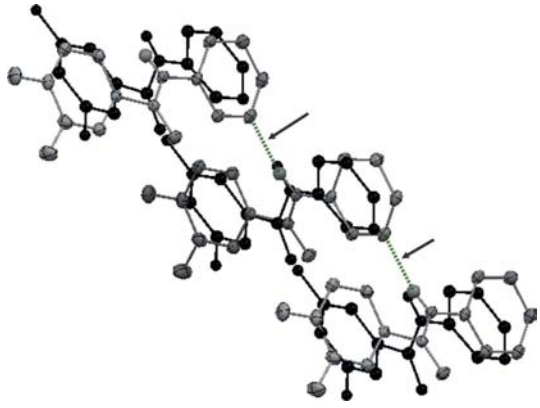

Figure 11
An overlay of (III) (grey) and (IV) (black), viewed along the [010] direction. Atoms in (III) are depicted as displacement ellipsoids at the 30% probability level and in (IV) using a ball-and-stick model. Only the amide H atoms are retained, and in (III) the short H···N interaction (2.143 Å) is highlighted with arrows.

benzene ring shows the largest C—C—C angles of 124 (1) and 123 (1)° at the 2,4-*ipso*-F sites [123.6 (2) and 123.2 (2)° in (I)], while the three smallest C—C—C angles are positioned *ortho* to the 2-/4-F atoms, with average CSD values of 116 (1), 117 (1) and 118 (1)° (Fig. 5). In (I) these angles are 116.5 (2) (at *Z*), 116.9 (2) and 117.7 (2)°. In the symmetrical 2,6-difluorobenzenes (Fig. 5), the *ipso*-F angles expand to 124 (2)° and the *ortho* angle (at *Z*) between the two C—F groups contracts to 115 (2)°. The two remaining *ortho* angles decrease to 118 (1)°. In both the 2,4-F_2 and 2,6-F_2 case studies, increasing C—F bond length correlates with increasing *ipso*-C—C—C angle (and *ortho*-C—C—C angle contracting from 120°). The symmetrical 3,5-difluorobenzenes (Fig. 5) and (IV) contrast remarkably with the 2,6-F_2 results in terms of angle changes relative to the *Z* group (Fig. 5). The *ipso* angles expand to 123 (2)° [123.74 (17) and 123.85 (17)° in (IV)] as the *ortho* C14 angle contracts to 116 (2)° [115.80 (17)° in (IV)], two *ortho* angles decrease to 118 (2) [118.37 (17) and 118.24 (17)° in (IV)] and there is a symmetrical 120 (2)° angle at C11 [120.00 (17)° in (IV)].

The CSD analyses and comparisons with (I) and (IV) serve to highlight distinct trends in how fluoro-aromatic substitution patterns affect the internal aromatic C—C—C angles in difluorobenzene fragments. It should be noted that there are no significant deviations from planarity in the C_6 (or C_5N) rings, with all C atoms within 0.01 Å of the mean plane. No trends are seen in the aromatic C—C bond lengths, nor are

they influenced by the fluoro substitution, although the aromatic C—C bond lengths are slightly shorter closer to the F-atom ring positions.

The hydrogen bonding in (I)–(IV) is of interest. Compounds (I) and (II) are isostructural at the primary hydrogen-bonding level but are not isomorphous. In both (I) and (II), intermolecular N—H···O=C interactions form one-dimensional chains along [010], with N···O^{i} = 3.017 (3) and 3.003 (2) Å, respectively (see Figs. 6 and 7 and Tables 1 and 2 for symmetry code). Pairs of molecules of (I) and (II) aggregate about inversion centres *via* centrosymmetric C—H···F interactions (see Tables 1 and 2). It is of note that the pyridyl N atom is not engaged in hydrogen bonding: the closest contacts are H···N$_{py}$ = 2.71 Å in (I) and 2.69 Å in (II). In (II), the closest π–π stacking interaction is C15···C26^{ii} = 3.243 (3) Å [symmetry code: (ii) $1-x, -y, 1-z$]. The overall effect is that the N—H···O=C one-dimensional chain is further linked into pairs *via* H···F interactions and forms a herring-bone network *via* weaker stacking, as stacked columns in (I) and side-by-side in (II).

A CSD search (Allen, 2002) was performed to analyse the types of interactions involving F atoms with H···F distances similar in magnitude to those in (I) and (II). Parameter restrictions were for C$_6$—H···F—C$_6$ with H···F = 1.0–2.5 Å and a C—H···F angle of 150–180° with coordinates, to yield a total of 117 hits (see second scheme). The interactions can be categorized as follows (and in combination): 85% as metal-containing, 84% with C$_6$F$_5$, 33% as salts and 59% as intramolecular interactions. Given that the C—H···F interaction in both (I) and (II) is organic and neutral, structures with comparable interactions of comparable dimensions are relatively uncommon, and examples include 7-(3,5-di-*tert*-butyldiphenyl)-2,12-bis(pentafluorophenyl)-5,6,8,9-tetrahydrodibenzo[*c*,*h*]acridine (CSD refcode CEDFOH; Korenaga *et al.*, 2005) and *trans*-[ethane-1,2-diamine-*N*,*N*′-bis(7-methylsalicylideneiminato)]di(2,4-difluorophenyldiboronate) (NERTIN; Sanchez *et al.*, 2001).

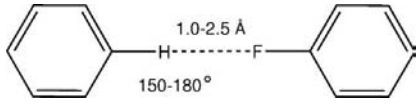

In (III), N—H···N$_{py}$ interactions form one-dimensional chains in tandem with a C—H···N$_{py}$ contact. C—H···O=C interactions about inversion centres form $R_2^2(10)$ rings. Molecules of (III) stack *via* π–π(arene) interactions about inversion centres. Closest C···ring distances are 3.38 and 3.44 Å, with *Cg*1···*Cg*2 = 3.574 (1) Å (*Cg*1 and *Cg*2 are the centroids of the C11–C16 and N24/C21–C23/C25/C26 rings, respectively). However, in (IV), there are no strong intermolecular interactions; the N—H···N$_{py}$ interaction is 0.3 Å longer than in (III) [N···N$_{py}$ = 3.272 (2) Å]. Weaker interactions include six C—H···N/O/F interactions, with H···N/O/F distances in the range 2.40 to 2.58 Å. The C=O group only participates in a weak interaction, with C···O = 3.225 (2) Å in (IV) [3.278 (2) Å in (III)]. The carbonyl group in (IV) is involved in three intermolecular interactions, with H···O distances in the range 2.40–2.58 Å. Differences between (III) and (IV) highlight the subtle interplay and competition between strong and weaker N—H···N$_{py}$ hydrogen bonding originating from subtle packing differences in their respective molecular structures.

The range in calculated densities of (I)–(IV) is 1.472–1.573 Mg m^{-3}, compared with an average of 1.53 Mg m^{-3} for all eight C$_{12}$H$_8$F$_2$N$_2$O compounds reported to date (McMahon *et al.*, 2008; Gallagher *et al.*, 2008), including the present study. It is of note that the lowest values of 1.465 and 1.472 Mg m^{-3} correspond to the 23*o* derivative (Gallagher *et al.*, 2008), which crystallizes with $Z' = 2$, and (III) or the 34*m* derivative, which is disordered in the C$_6$ ring.

Experimental

For the preparation of (I)–(IV) (Fink & Kurys, 1996), typically, the 2,4-, 2,5-, 3,4- and 3,5-difluorobenzoyl chloride (10 mmol) in dry CH_2Cl_2 (20–30 ml) was added dropwise over a period of 2–3 min to a cold (273 K) 20–30 ml solution of 3-aminopyridine in chloroform containing Et_3N (1.5 ml), and the reaction was stirred overnight at room temperature. Typical organic work-up and washings furnished the products in reasonable yields of 40–90%. Crystals suitable for diffraction were grown from $CHCl_3$ as colourless blocks over a period of 1–2 weeks. Compounds (I)–(IV) gave clean ^{1}H and ^{13}C NMR spectra in d_6-DMSO and the IR spectra (in $CHCl_3$ solution or as KBr discs) are as expected and are available in the archived CIF.

Compound (I)

Crystal data

C$_{12}$H$_8$F$_2$N$_2$O
M_r = 234.20
Monoclinic, $P2_1/n$
a = 13.9692 (5) Å
b = 5.0957 (2) Å
c = 15.3151 (8) Å
β = 113.812 (2)°
V = 997.37 (8) Å^3
Z = 4
Mo $K\alpha$ radiation
μ = 0.13 mm^{-1}
T = 150 K
0.30 × 0.20 × 0.15 mm

Data collection

Nonius KappaCCD diffractometer
Absorption correction: multi-scan (*SORTAV*; Blessing, 1995)
T_{min} = 0.963, T_{max} = 0.975
5121 measured reflections
2269 independent reflections
1247 reflections with $I > 2\sigma(I)$
R_{int} = 0.092

Refinement

$R[F^2 > 2\sigma(F^2)]$ = 0.056
$wR(F^2)$ = 0.170
S = 1.02
2269 reflections
158 parameters
H atoms treated by a mixture of independent and constrained refinement
$\Delta\rho_{max}$ = 0.27 e Å^{-3}
$\Delta\rho_{min}$ = −0.34 e Å^{-3}

Compound (II)

Crystal data

C$_{12}$H$_8$F$_2$N$_2$O
M_r = 234.20
Monoclinic, $P2_1/c$
a = 8.0371 (7) Å
b = 5.1425 (4) Å
c = 23.994 (2) Å
β = 94.320 (4)°
V = 988.87 (15) Å^3
Z = 4
Mo $K\alpha$ radiation
μ = 0.13 mm^{-1}
T = 150 K
0.20 × 0.18 × 0.05 mm

Data collection

Nonius KappaCCD diffractometer
Absorption correction: multi-scan (*SORTAV*; Blessing, 1995)
T_{min} = 0.724, T_{max} = 0.999
5500 measured reflections
2181 independent reflections
1346 reflections with $I > 2\sigma(I)$
R_{int} = 0.061

Refinement

$R[F^2 > 2\sigma(F^2)]$ = 0.052
$wR(F^2)$ = 0.146
S = 1.02
2181 reflections
159 parameters
H atoms treated by a mixture of independent and constrained refinement
$\Delta\rho_{max}$ = 0.26 e Å^{-3}
$\Delta\rho_{min}$ = −0.22 e Å^{-3}

Compound (III)

Crystal data

$C_{12}H_8F_2N_2O$
M_r = 234.20
Monoclinic, $P2_1/n$
a = 7.6741 (5) Å
b = 13.7314 (6) Å
c = 10.3316 (8) Å
β = 103.861 (3)°
V = 1057.00 (12) Å^3
Z = 4
Mo $K\alpha$ radiation
μ = 0.12 mm^{-1}
T = 150 K
0.26 × 0.24 × 0.12 mm

Data collection

Nonius KappaCCD diffractometer
Absorption correction: multi-scan (*SORTAV*; Blessing, 1995)
T_{min} = 0.884, T_{max} = 0.987
7204 measured reflections
2412 independent reflections
1512 reflections with $I > 2\sigma(I)$
R_{int} = 0.048

Refinement

$R[F^2 > 2\sigma(F^2)]$ = 0.050
$wR(F^2)$ = 0.142
S = 1.05
2412 reflections
169 parameters
1 restraint
H atoms treated by a mixture of independent and constrained refinement
$\Delta\rho_{max}$ = 0.22 e Å^{-3}
$\Delta\rho_{min}$ = −0.23 e Å^{-3}

Compound (IV)

Crystal data

$C_{12}H_8F_2N_2O$
M_r = 234.20
Monoclinic, $P2_1/n$
a = 8.3784 (5) Å
b = 12.6278 (8) Å
c = 9.9118 (5) Å
β = 101.152 (3)°
V = 1028.87 (10) Å^3
Z = 4
Mo $K\alpha$ radiation
μ = 0.12 mm^{-1}
T = 150 K
0.22 × 0.20 × 0.18 mm

Data collection

Nonius KappaCCD diffractometer
Absorption correction: multi-scan (*SORTAV*; Blessing, 1995)
T_{min} = 0.938, T_{max} = 0.983
7054 measured reflections
2348 independent reflections
1535 reflections with $I > 2\sigma(I)$
R_{int} = 0.046

Refinement

$R[F^2 > 2\sigma(F^2)]$ = 0.051
$wR(F^2)$ = 0.141
S = 1.03
2348 reflections
159 parameters
H atoms treated by a mixture of independent and constrained refinement
$\Delta\rho_{max}$ = 0.27 e Å^{-3}
$\Delta\rho_{min}$ = −0.24 e Å^{-3}

Compounds (I) and (II) are isostructural and in the same space group [$P2_1/n$ for (I) and $P2_1/c$ for (II); No. 14]. They differ by >10% in their a and c unit-cell dimensions. Conversion of (I) from $P2_1/n$ to a $P2_1/c$ setting gives a = 13.97, b = 5.09, c = 16.03 Å and β = 119.06°, different to the values of a = 8.04, b = 5.14, c = 23.99 Å and β = 94.32° for (II). Compounds (III) and (IV) (in $P2_1/n$) differ by 9% on the a and b dimensions and 4% on the c-axis length, but they are essentially isomorphous, as the a and b unit-cell differences can be attributed to the effects of the peripheral F-atom substitution and disorder patterns.

H atoms attached to C atoms were treated as riding using the *SHELXL97* (Sheldrick, 2008) defaults at 150 (1) K, with C—H = 0.95 Å and U_{iso}(H) = 1.2U_{eq}(C). N-bound H atoms were refined freely with isotropic displacement parameters.

Rotational disorder is present in the difluorophenyl group in (III), with site-occupancy factors of 0.809 (4) and 0.191 (4), respectively, for the major and minor components of disorder. As both C_6 atom sites in both rings overlay and occupy the same space, only the F/H atoms were treated in the disorder. The C—F bond length for the minor F-atom site was restrained to 1.350 (5) Å.

The extinction coefficient refines to 0.006 (3) in (I), 0.015 (5) in (II), 0.017 (6) in (III) and 0.014 (5) in (IV). Refinement for (I) was

Table 1
Hydrogen-bond geometry (Å, °) for (I).

D—H···A	D—H	H···A	D···A	D—H···A
N1—H1···F12	0.86 (3)	2.24 (3)	2.741 (3)	117 (2)
N1—H1···O1^{i}	0.86 (3)	2.20 (3)	3.017 (3)	158 (3)
C26—H26···O1	0.95	2.41	2.911 (3)	113
C22—H22···F12^{ii}	0.95	2.43	3.360 (3)	168

Symmetry codes: (i) $x, y-1, z$; (ii) $-x+1, -y, -z$.

Table 2
Hydrogen-bond geometry (Å, °) for (II).

D—H···A	D—H	H···A	D···A	D—H···A
N1—H1···F12	0.89 (3)	2.14 (3)	2.726 (2)	123 (2)
N1—H1···O1^{i}	0.89 (3)	2.22 (3)	3.003 (2)	148 (2)
C26—H26···O1	0.95	2.40	2.913 (3)	113
C22—H22···F12^{ii}	0.95	2.43	3.339 (3)	161

Symmetry codes: (i) $x, y+1, z$; (ii) $-x, -y+1, -z+1$.

Table 3
Hydrogen-bond geometry (Å, °) for (III).

D—H···A	D—H	H···A	D···A	D—H···A
N1—H1···N23^{i}	0.87 (2)	2.14 (2)	2.990 (2)	164.2 (17)
C12—H12···O1^{ii}	0.95	2.36	3.278 (2)	162
C16—H16···N23^{i}	0.95	2.51	3.334 (2)	146

Symmetry codes: (i) $x-\frac{1}{2}, -y+\frac{1}{2}, z-\frac{1}{2}$; (ii) $-x+2, -y+1, -z+1$.

Table 4
Hydrogen-bond geometry (Å, °) for (IV).

D—H···A	D—H	H···A	D···A	D—H···A
N1—H1···N23^{i}	0.89 (2)	2.41 (2)	3.272 (2)	164.5 (18)
C22—H22···O1	0.95	2.21	2.799 (2)	119
C12—H12···O1^{ii}	0.95	2.40	3.225 (2)	144
C16—H16···N23^{i}	0.95	2.46	3.381 (2)	163
C14—H14···O1^{iii}	0.95	2.58	3.482 (2)	158
C24—H24···O1^{iv}	0.95	2.48	3.420 (2)	170
C25—H25···F15^{v}	0.95	2.52	3.120 (2)	121
C26—H26···F15^{v}	0.95	2.52	3.117 (2)	121

Symmetry codes: (i) $x-\frac{1}{2}, -y+\frac{1}{2}, z-\frac{1}{2}$; (ii) $-x+2, -y+1, -z+1$; (iii) $-x+\frac{3}{2}, y+\frac{1}{2}, -z+\frac{1}{2}$; (iv) $-x+\frac{3}{2}, y-\frac{1}{2}, -z+\frac{3}{2}$; (v) $-x+\frac{1}{2}, y-\frac{1}{2}, -z+\frac{1}{2}$.

Table 5
Comparison of selected torsion/dihedral angles (°) in (I)–(IV).

Angle	(I)	(II)	(III)	(IV)
O1—C1—N1—C21	8.7 (4)	8.8 (4)	1.8 (3)	−2.1 (3)
O1—C1—C11—C12	−152.1 (3)	−153.7 (2)	18.0 (2)	−18.6 (2)
C11—C1—N1—C21	−171.8 (2)	−172.0 (2)	−177.69 (15)	178.88 (15)
C1—N1—C21—C22	153.3 (2)	153.9 (2)	−23.6 (2)	20.7 (3)
Benzene–pyridine	4.48 (18)	3.66 (11)	3.63 (11)	2.94 (11)
Benzene–amide	27.3 (3)	25.39 (10)	18.64 (25)	20.0 (2)
Pyridine–amide	23.3 (4)	22.23 (11)	21.6 (2)	18.0 (2)
C—C(F)—C†	123.6 (2)	123.8 (2)	120.88 (18)	123.74 (17)
C—C(F)—C†	123.3 (2)	123.1 (2)	120.45 (17)	123.85 (17)

† *ipso* angle (internal) at the F-substituted C atom.

finalized with no correction, while for (II)–(IV), since they have corrections which are just significant at the 3σ level, this correction was retained.

For all compounds, data collection: *KappaCCD Server Software* (Nonius, 1997); cell refinement: *DENZO-SMN* (Otwinowski & Minor, 1997); data reduction: *DENZO-SMN*; program(s) used to solve structure: *SHELXS97* (Sheldrick, 2008); program(s) used to refine structure: *SHELXL97* (Sheldrick, 2008) and *SORTX* (McArdle, 1995); molecular graphics: *PLATON* (Spek, 2009); software used to prepare material for publication: *SHELXL97* and *PREP8* (Ferguson, 1998).

JFG thanks Dublin City University for grants in aid of undergraduate research. Thanks are due especially to Mr Damien McGuirk for providing excellent technical assistance in the undergraduate research laboratories at DCU.

Supplementary data for this paper are available from the IUCr electronic archives (Reference: SK3328). Services for accessing these data are described at the back of the journal.

References

Allen, F. H. (2002). *Acta Cryst.* B**58**, 380–388.
Bernstein, J., Davis, R. E., Shimoni, L. & Chang, N.-L. (1995). *Angew. Chem. Int. Ed. Engl.* **34**, 1555–1573.
Blessing, R. H. (1995). *Acta Cryst.* A**51**, 33–38.
Chopra, D. & Row, T. N. G. (2008). *CrystEngComm*, **10**, 54–67.
Donnelly, K., Gallagher, J. F. & Lough, A. J. (2008). *Acta Cryst.* C**64**, o335–o340.
Ferguson, G. (1998). *PREP8*. University of Guelph, Canada.
Fink, D. M. & Kurys, B. E. (1996). *Tetrahedron Lett.* **37**, 995–998.
Gallagher, J. F., McMahon, J., Anderson, F. P. & Lough, A. J. (2008). *Acta Cryst.* E**64**, o2394.
Gelbrich, T., Hursthouse, M. B. & Threlfall, T. L. (2007). *Acta Cryst.* B**63**, 621–632.
Gowda, B. T., Foro, S., Babitha, K. S. & Fuess, H. (2008). *Acta Cryst.* E**64**, o1390.
Gowda, B. T., Foro, S., Sowmya, B. P. & Fuess, H. (2008). *Acta Cryst.* E**64**, o383.
Klösener, J., Swenson, D. C., Robertson, L. W. & Luthe, G. (2008). *Acta Cryst.* B**64**, 108–119.
Korenaga, T., Kawauchi, Y., Kosaki, T., Ema, T. & Sakai, T. (2005). *Bull. Chem. Soc. Jpn*, **78**, 2175–2179.
Luthe, G., Swenson, D. C. & Robertson, L. W. (2007). *Acta Cryst.* B**63**, 319–327.
McArdle, P. (1995). *J. Appl. Cryst.* **28**, 65.
McMahon, J., Anderson, F. P., Gallagher, J. F. & Lough, A. J. (2008). *Acta Cryst.* C**64**, o493–o497.
Nonius (1997). *KappaCCD Server Software*. Windows 3.11 Version. Nonius BV, Delft, The Netherlands.
Otwinowski, Z. & Minor, W. (1997). *Methods in Enzymology*, Vol. 276, *Macromolecular Crystallography*, Part A, edited by C. W. Carter Jr & R. M. Sweet, pp. 307–326. New York: Academic Press.
Sanchez, M., Hopfl, H., Ochoa, M.-E., Frafan, N., Santillan, R. & Rojas, S. (2001). *Inorg. Chem.* **40**, 6405–6412.
Shao, Y. *et al.* (2006). *Phys. Chem. Chem. Phys.* **8**, 3172–3191.
Sheldrick, G. M. (2008). *Acta Cryst.* A**64**, 112–122.
Spek, A. L. (2009). *Acta Cryst.* D**65**, 148–155.
Threlfall, T. L. & Gelbrich, T. (2007). *Cryst. Growth Des.* **7**, 2297.
Wardell, S. M. S. V., de Souza, M. V. N., Vasconcelos, T. R. A., Ferreira, M. L., Wardell, J. L., Low, J. N. & Glidewell, C. (2008). *Acta Cryst.* B**64**, 84–100.
Wardell, S. M. S. V., de Souza, M. V. N., Wardell, J. L., Low, J. N. & Glidewell, C. (2007). *Acta Cryst.* B**63**, 879–895.